

INTERFEROMETRIC PHASE CALIBRATION SOURCES  
IN THE DECLINATION RANGE  $0^\circ$  TO  $-30^\circ$

JOSHUA N. WINN<sup>1,2</sup>, ALOK R. PATNAIK<sup>3,4</sup>, J.M. WROBEL<sup>5</sup>

ABSTRACT

We present a catalog of 321 compact radio sources in the declination range  $0^\circ > \delta > -30^\circ$ . The positions of these sources have been measured with a two-dimensional rms accuracy of 35 milliarcseconds using the NRAO<sup>a</sup> Very Large Array. Each source has a peak flux density  $> 50$  mJy at 8.4 GHz. We intend for this catalog to be used mainly for selection of phase calibration sources for radio interferometers, although compact radio sources have other scientific uses.

<sup>a</sup> The National Radio Astronomy Observatory is a facility of the National Science Foundation operated under cooperative agreement by Associated Universities, Inc.

*Subject headings:* astrometry — catalogs — radio continuum — techniques: interferometric

1. INTRODUCTION

Radio interferometers measure the amplitudes and phases of Fourier components of the sky brightness distribution. The phases are generally more susceptible than the amplitudes to corruption due to the electronics and the atmosphere. Yet the phases encode important information about the position and structure of the radio source. For bright sources, the phases can be corrected by means of self-calibration (Pearson & Readhead 1984). When the source is too faint for self-calibration, or when the absolute position of the source is desired, it is essential to correct the phase errors with frequent observations of a reference source, or “phase calibrator.” To be useful, a phase calibrator should be bright, have an accurately determined position, and exhibit a simple (preferably compact) radio structure. A phase calibrator should also be separated from the target source by as small a switching angle as possible, to minimize differential atmospheric phase errors. This makes it valuable to identify a dense grid of phase calibrators across the sky.

For historical reasons, the southern sky is not as well-explored for phase calibrators as the northern sky. In this paper we help redress this imbalance by presenting a catalog of 321 compact radio sources in the declination range  $0^\circ > \delta > -30^\circ$ . The positions in the catalog have a two-dimensional root-mean-squared (rms) accuracy of 35 milliarcseconds (mas). Our catalog is derived from observations with the NRAO Very Large Array (VLA) that were very similar in technique to those employed by the Jodrell Bank–VLA Astrometric Survey (JVAS: Patnaik et al. 1992; Browne et al. 1998; Wilkinson et al. 1998). Our new observations are described in § 2. The details of data reduction, including the determination of the accuracy of the derived positions, are given in § 3. The catalog is presented in § 4. In the paper version of this article, only the first page of the catalog is reproduced; the entire catalog

can be found in the electronic version of this article. In § 5 we summarize and highlight other possible uses of the catalog.

2. OBSERVATIONS

In general, the structure of a radio source with a flat spectral index ( $\alpha \geq -0.5$ , where  $S_\nu \propto \nu^\alpha$ ) is dominated by a core that is compact on milliarcsecond scales. This was the underlying assumption of our strategy for selecting potential phase calibrators, as it was with JVAS.

We selected flat-spectrum sources in the region  $0^\circ > \delta_{\text{B1950}} > -30^\circ$ , using the Parkes catalogs (PKS; Otrupcek & Wright 1991) and early versions of the Parkes–MIT–NRAO catalogs (PMN; since published by Griffith & Wright 1993; Griffith et al. 1994, 1995; Wright et al. 1996). For the PKS sources, we required  $S_{2.7 \text{ GHz}} > 150$  mJy and computed spectral indices between 0.4 GHz and 2.7 GHz, or between 2.7 GHz and 5.0 GHz, depending on the information available in the Parkes catalogs. For the PMN sources, we required  $S_{4.9 \text{ GHz}} > 120$  mJy and computed spectral indices between the 4.9 GHz PMN measurement and the 2.7 GHz Parkes measurement. These flat-spectrum targets, 719 in total, typically had positions with a two-dimensional rms accuracy of  $16''$ . Confusion from Galactic emission, particularly when spectral indices involved a 0.4 GHz measurement, led to a zone of avoidance around the Galactic plane.

We used the VLA (Thompson et al. 1980) to observe these sources for a total of 63 hours, in four separate sessions during the period 1994 February 20–24 UT. At this time, the array was being changed from its most compact configuration (D) to its most extended configuration (A). For our observations most of the antennas were in their A-configuration positions, but a few antennas (no more than 7) were still in their D-configuration positions.

Data were acquired in dual circular polarizations at a center frequency of 8.43 GHz and with a bandwidth of

<sup>1</sup> Harvard-Smithsonian Center for Astrophysics, 60 Garden St., Cambridge, MA 02138

<sup>2</sup> NSF Astronomy & Astrophysics Postdoctoral Fellow

<sup>3</sup> Max-Planck-Institut für Radioastronomie, Auf dem Hügel 69, 53121 Bonn, Germany

<sup>4</sup> present address: Apt. 1703, 1435 Prince of Wales Drive, Ottawa K2C 1N5, Canada

<sup>5</sup> National Radio Astronomy Observatory, P.O. Box 0, Socorro, NM 87801

25 MHz. We did not use the full 50 MHz bandwidth that is routinely available, in order to minimize bandwidth smearing of the target sources. (For sources as bright as our target sources, the error in the derived positions is dominated by systematic effects such as bandwidth smearing, rather than statistical error.) Observations were made assuming a coordinate equinox of 2000.

Our phase calibrators for these observations were sources for which positions had been measured with very-long-baseline interferometry (VLBI) in the early 1990s, with an accuracy of approximately 2 mas (see Russell et al. 1994, and references therein). The phase calibrators that we used, and the VLBI positions we assumed for them, are listed in Table 1. This table excludes the sources that we intended to use as phase calibrators but that proved to be too resolved for this purpose, as described in § 3.

We observed an additional 26 sources drawn from Russell et al. (1994), but did not use these 26 sources as phase calibrators, in order to quantify the astrometric accuracy of our observations. These “astrometric check sources” were treated exactly the same as target sources during the observations and data reduction. A list of the astrometric check sources, and the VLBI-based positions we assumed for them, is given in Table 2.

All sources in our program (targets, calibration sources, and astrometric check sources) were scheduled for 2-minute observations. The switching time between phase calibrator observations was 6 minutes, with switching angles that were usually less than  $10^\circ$  (but occasionally up to  $15^\circ$ ). After allowing time for telescope slewing, and electronics settling, this provided 1–1.5 minutes of integration time per observation per source. Additional observations of the primary flux density calibrator 3C286 (= J1331+3030) were used to set the flux density scale to an accuracy of approximately 3%. Information on all Stokes parameters was obtained, but this paper presents the results for Stokes  $I$  only.

### 3. DATA REDUCTION

The data were calibrated with the NRAO AIPS<sup>6</sup> software, using standard procedures. At this stage we recognized that some of our intended phase calibrators had structure that was significantly resolved by the VLA. These poor phase calibrators do not appear in Table 1. We also excluded from further analysis all targets that were meant to have been calibrated by these poor phase calibrators.

As an internal consistency check, the positions and structures of the targets were determined using two completely different methods, described below. We stress that, in both methods, the centroid positions for the targets were derived prior to any self-calibration.

The first method, identical to that employed by Patnaik et al. (1992), Browne et al. (1998), and Wilkinson et al. (1998) for JVAS, used an automatic procedure in AIPS that located the target within a wide-field ( $82''$ ) map and determined its position by fitting a quadratic profile to the brightest component in the map. The source structure was then determined by creating a smaller map ( $20''$ ) and performing two iterations of CLEAN and phase-only self-calibration. The synthesized beam, using uniform weight-

ing, was typically  $0''.4 \times 0''.2$ . The peak flux density in the final map was recorded, along with the total flux density within a  $10'' \times 10''$  region centered on the peak.

The second method, similar to that employed by Myers et al. (2002) and Winn (2001) for gravitational lens surveys with the VLA, used an automatic procedure in DIFMAP (Shepherd, Pearson, & Taylor 1994) that located the target within a wide-field map ( $128''$ ) and determined its position by fitting a point-source model to the visibility data in Fourier space. The source structure was then determined by creating a smaller map ( $25''$ ) and performing iterations of CLEAN and phase-only self-calibration until prescribed limits on dynamic range or map noise had been achieved. The synthesized beam, using uniform weighting, was typically  $0''.4 \times 0''.2$ . The peak flux density in the final map, and the total flux density in the CLEAN model, were recorded.

We also inspected a plot of visibility amplitude *versus* baseline length for each target, and discarded targets for which the data appeared suspicious, whether because of gross resolution, bandwidth smearing, confusion, or obviously corrupted data. All surviving targets were then filtered for adequate brightness ( $S_{8.4 \text{ GHz}}^{\text{peak}} > 50 \text{ mJy beam}^{-1}$ ) and compactness ( $S_{8.4 \text{ GHz}}^{\text{total}} < 1.2 \times S_{8.4 \text{ GHz}}^{\text{peak}}$ ). For those bright and compact targets, the rms differences between the coordinates derived using the two different data-analysis methods were 8 mas in right ascension and 10 mas in declination. There were four extreme outliers with two-dimensional positions differing by more than 50 mas; those four targets were discarded.

After all of these quality-control filters had been applied, a total of 321 bright and compact targets remained. The locations of these targets are shown in Fig. 1, in which the Galactic zone of avoidance is evident. The positions and flux densities of these 321 targets are presented in Table 3. The tabulated entries are those derived from the DIFMAP-based analysis.

As an external test of astrometric accuracy, we measured the positions of the astrometric check sources using exactly the same DIFMAP-based analysis as used for the target sources. The rms differences between our VLA-based coordinates and the VLBI-based coordinates are 19 mas in right ascension and 21 mas in declination, implying a two-dimensional rms accuracy of 28 mas. The differences between the VLBI positions and the VLA positions are plotted in Fig. 2.

A second external test of astrometric accuracy has recently become possible, because many of the targets in a preliminary version of our catalog were subsequently observed with the Very Long Baseline Array (VLBA) as part of the VLBA Calibrator Survey (VCS; Beasley et al. 2002). The median one-dimensional uncertainty in the VCS1 positions (along the major axis of the error ellipse) is 0.9 mas. The VCS1 catalog contains 201 sources in common with Table 3 of this paper. These sources are identified by the comment “VCS1” in Table 3. The rms differences between our VLA-based coordinates and the VCS1 coordinates are 22 mas in right ascension and 27 mas in declination, implying a two-dimensional rms accuracy of 35 mas. The differences between the VLBI positions and the VLA positions are plotted in Fig. 3. Based on this analysis, we

<sup>6</sup> The Astronomical Image Processing System (AIPS) is developed and distributed by the NRAO.

estimate the two-dimensional rms error of our catalog to be 35 mas.

#### 4. THE CATALOG

The positions and flux densities of the 321 new phase calibrators found from our VLA observations are given in Table 3. These entries are derived from the DIFMAP-based analysis, rather than the AIPS-based analysis, although, as mentioned in the previous section, the agreement between the two methods was excellent. The columns of Table 3 contain the following information:

- Col. 1. Source name derived from J2000 coordinates,
- Col. 2. Right ascension (hours, minutes, seconds) in J2000 coordinates,
- Col. 3. Declination (degrees, arcminutes, arcseconds) in J2000 coordinates,
- Col. 4. Total flux density  $S_{8.4\text{ GHz}}^{\text{total}}$  in mJy,
- Col. 5. Peak flux density  $S_{8.4\text{ GHz}}^{\text{peak}}$  in mJy beam<sup>-1</sup>,
- Col. 6. Comment.

The comment “VCS1” in the sixth column indicates that the source was subsequently observed by Beasley et al. (2002) and appears in the VLBA Calibrator Survey-1 catalog. The positions in the VCS1 catalog generally have a much smaller uncertainty ( $\sim 1$  mas), and are preferable to our positions when selecting a phase calibrator for VLBI observations.

The catalog contains a few sources with declinations slightly larger than  $0^\circ$  because the selection was originally performed in B1950 coordinates. It is important to note that the catalog is not a complete sample of compact sources in the stated declination range. While we did observe a statistically complete sample of flat-spectrum sources, the catalog presents only the subset of sources that survived our very conservative quality-control filters.

In the paper version of this article, only the first page of the table is reproduced, as an example. The entire table is available in the electronic version of this paper.

#### 5. SUMMARY AND DISCUSSION

We have produced a new catalog of compact radio sources in a dense grid in the southern sky. The catalog is intended to be useful for selecting phase calibration sources for radio interferometers, which is why we took special care in estimating the astrometric accuracy of the

positions, and in discarding data that were suspect in any way. These compact radio sources can be used as phase calibration sources and also as positional references for proper-motion studies of nearby objects.

Compact sources can also be utilized in other ways. First, sources with intrinsically small angular sizes are required to study scintillation, angular broadening, and Faraday rotation due to the interstellar or interplanetary medium (see, e.g., Rickett 1990, 2001, for reviews). Second, some compact sources exhibit intra-day variability, a topic of intense recent interest (see, e.g., Jauncey et al. 2001). Third, those few compact sources that have stable flux densities, such as gigahertz-peaked-spectrum sources (GPS; see, e.g., O’Dea 1998) and especially compact symmetric objects (Fassnacht & Taylor 2001), can be used as convenient flux density standards. These sources are rare, but the compact sources in our catalog can be investigated for this purpose.

Finally, the observing methods described in this article—snapshot surveys of hundreds of flat-spectrum sources—have also proven useful for finding gravitational lenses. Lenses are fairly easy to recognize in these surveys, because they have multiple compact components separated by  $\sim 0'.5\text{--}6''$ , unlike the great majority of flat-spectrum sources. This technique was used by JVAS (King et al. 1999) and CLASS (Myers et al. 2002; Browne et al. 2002) to find dozens of new cases of multiple-image gravitational lensing. Moreover, Winn (2001) has used the data described in this paper, along with other VLA data, to discover 4 new lenses to date (Winn et al. 2000, 2001, 2002a, 2002b). The details of that lens survey, and the reduction of those other VLA data, will be described in a future paper. The subset of the observations presented here was designed especially for astrometric accuracy, unlike those other observations, and thus merited separate treatment.

We thank I. Browne and P. Wilkinson for a productive collaboration on JVAS in the northern sky and for useful discussions. We are also grateful to J. Russell for providing updated positions for VLBI sources in advance of our observations; to S. Myers and C. Fassnacht for assistance with DIFMAP; and to D. Rusin for comments on the manuscript. J.N.W. is supported by an Astronomy & Astrophysics Postdoctoral Fellowship, under NSF grant AST-0104347.

#### REFERENCES

- Beasley, A.J., et al. 2002, *ApJS*, 141, 13
- Browne, I.W.A., Patnaik, A.R., Wilkinson, P.N., & Wrobel, J.M. 1998, *MNRAS*, 293, 257
- Browne, I.W.A., et al. 2002, *MNRAS*, submitted
- Fassnacht, C.D. & Taylor, G.B. 2001, *AJ*, 122, 1661
- Griffith, M.R. & Wright, A.E. 1993, *AJ*, 105, 1666
- Griffith, M.R., Wright, A.E., Burke, B.F., & Ekers, R.D. 1994, *ApJS*, 90, 179
- Griffith, Mark R., Wright, Alan E., Burke, B.F., & Ekers, R.D. 1995, *ApJS*, 97, 347
- Jauncey, D.L., et al. 2001, *Ap&SS*, 278, 87
- King, L.J., et al. 1999, *MNRAS*, 307, 225
- Myers, S.T., et al. 2002, *MNRAS*, submitted
- O’Dea, C.P. 1998, *PASP*, 110, 493
- Otrupcek, R.E. & Wright, A.E. 1991, *Proc. Astr. Soc. Aust.* 9, 170
- Patnaik, A.R., Browne, I.W.A., Wilkinson, P.N., & Wrobel, J.M. 1992, *MNRAS*, 254, 655
- Pearson, T.J. & Readhead, A.C.S. 1984, *ARA&A*, 22, 97
- Rickett, B.J. 1990, *ARA&A*, 28, 561
- Rickett, B.J. 2001, *Ap&SS*, 278, 5
- Russell, J.L., et al. 1994, *AJ*, 107, 379
- Shepherd, M.C., Pearson, T.J. & Taylor, G.B. 1994, *BAAS*, 27, 903
- Thompson, A.R., Clark, B.G., Wade, C.M., & Napier, P.J. 1980, *ApJS*, 44, 151
- Wilkinson, P.N., Browne, I.W.A., Patnaik, A.R., Wrobel, J.M., & Sorathia, B. 1998, *MNRAS*, 300, 790
- Winn, J.N., Ph.D. thesis, Massachusetts Institute of Technology
- Winn, J.N., et al. 2000, *AJ*, 120, 2868
- Winn, J.N., et al. 2001, *AJ*, 121, 1223
- Winn, J.N., et al. 2002, *ApJ*, 564, 143
- Winn, J.N., et al. 2002, *AJ*, 123, 10
- Wright, A.E., Griffith, M.R., Hunt, A.J., Troup, E., Burke, B.F. & Ekers, R.D. 1996, *ApJS*, 103, 145

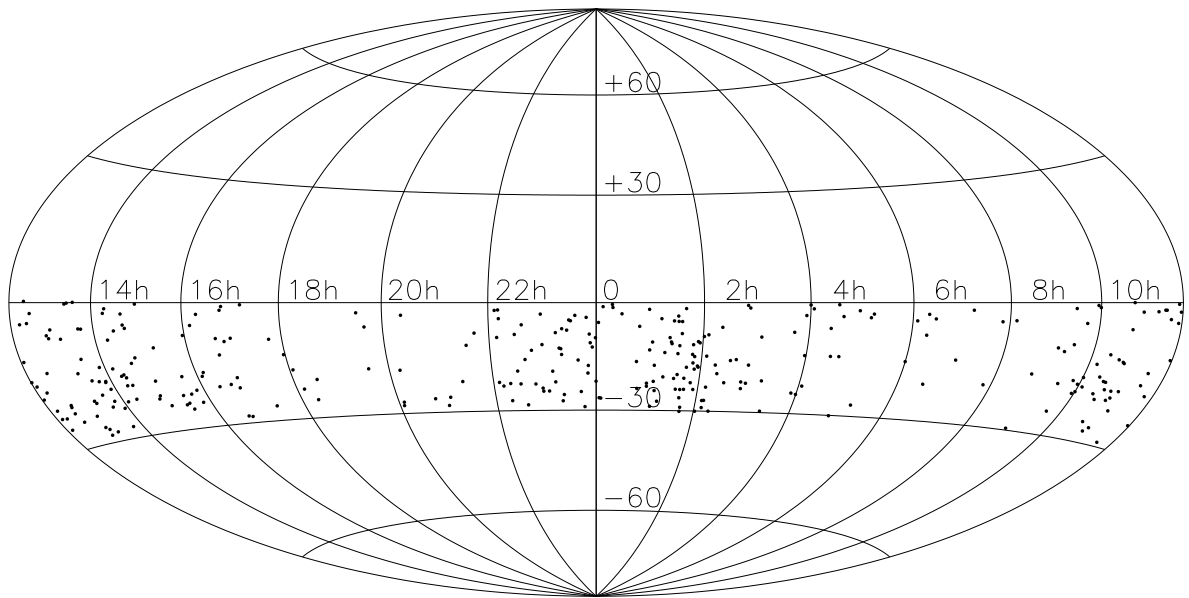


FIG. 1.— Celestial coordinates of the 321 compact radio sources given in Table 3, shown on an Aitoff equal-area projection.

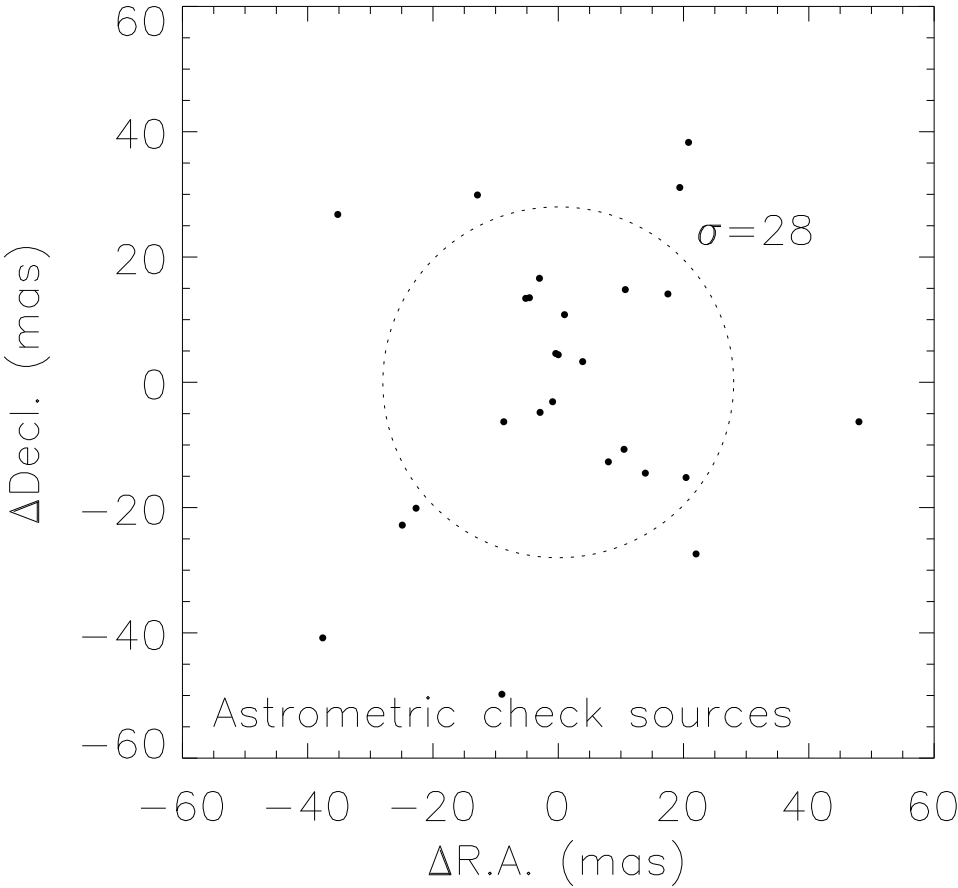


FIG. 2.— Differences between the positions derived from our VLA observations and the VLBI-based positions for the 26 astrometric check sources. The two-dimensional rms of 28 mas is indicated by the dotted circle.

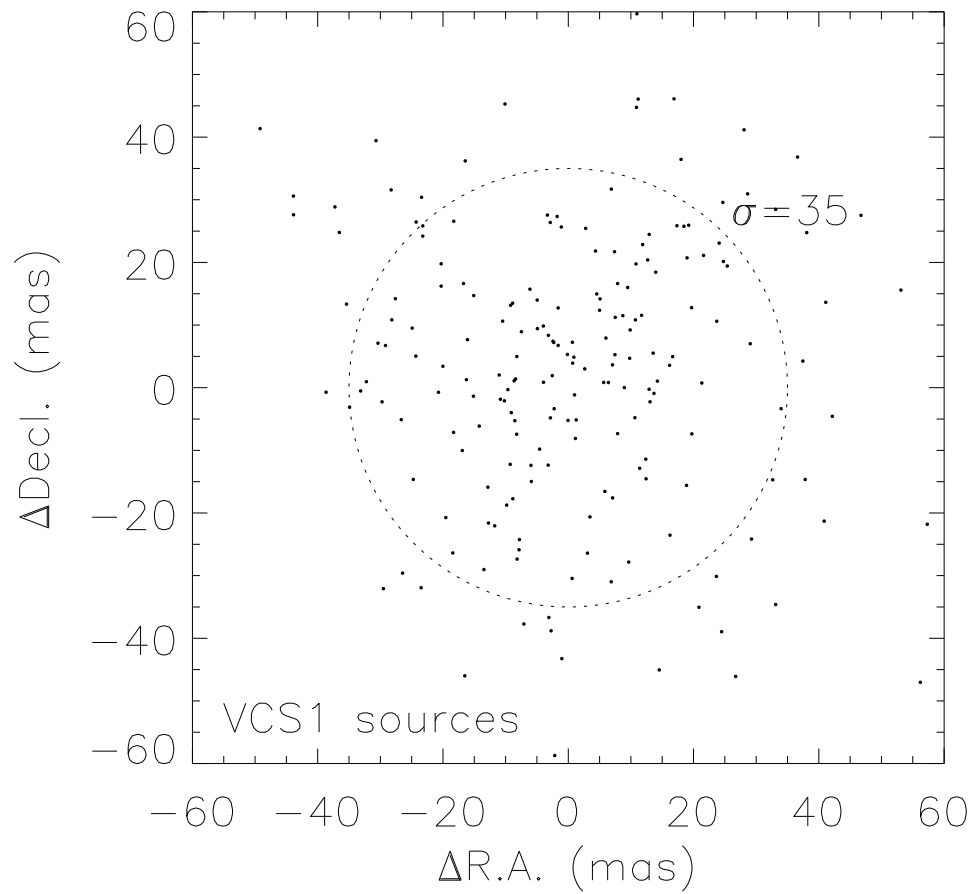


FIG. 3.— Differences between the positions derived from our VLA observations and the VCS1 positions for the 201 sources in common between our catalog and VCS1. The two-dimensional rms of 35 mas is indicated by the dotted circle. Ten sources are missing from this plot because one or both coordinate differences exceed 60 mas.

TABLE 1  
PHASE CALIBRATION SOURCES AND THEIR ASSUMED POSITIONS.

J2000 Name	Right Ascension (J2000)	Declination (J2000)
J0006-0623	00:06:13.8929	-06:23:35.334
J0011-2612	00:11:01.2467	-26:12:33.376
J0016-0015	00:16:11.0885	-00:15:12.444
J0050-0929	00:50:41.3174	-09:29:05.209
J0113+0222	01:13:43.1449	+02:22:17.317
J0116-1136	01:16:12.5220	-11:36:15.433
J0120-2701	01:20:31.6634	-27:01:24.651
J0137-2430	01:37:38.3463	-24:30:53.884
J0141-0928	01:41:25.8321	-09:28:43.673
J0204-1701	02:04:57.6743	-17:01:19.839
J0217+0144	02:17:48.9548	+01:44:49.700
J0240-2309	02:40:08.1745	-23:09:15.731
J0241-0815	02:41:04.7984	-08:15:20.752
J0339-0146	03:39:30.9378	-01:46:35.803
J0340-2119	03:40:35.6079	-21:19:31.170
J0416-1851	04:16:36.5445	-18:51:08.339
J0423-0120	04:23:15.8007	-01:20:33.064
J0442-0017	04:42:38.6608	-00:17:43.418
J0453-2807	04:53:14.6469	-28:07:37.326
J0457-2324	04:57:03.1792	-23:24:52.019
J0501-0159	05:01:12.8099	-01:59:14.255
J0530-2503	05:30:07.9628	-25:03:29.898
J0539-1550	05:39:32.0101	-15:50:30.319
J0607-0834	06:07:59.6992	-08:34:49.977
J0730-1141	07:30:19.1124	-11:41:12.599
J0739+0137	07:39:18.0339	+01:37:04.619
J0745-0044	07:45:54.0823	-00:44:17.539
J0811+0146	08:11:26.7073	+01:46:52.221
J0826-2230	08:26:01.5730	-22:30:27.203
J0902-1415	09:02:16.8309	-14:15:30.874
J0909+0121	09:09:10.0916	+01:21:35.618
J0921-2618	09:21:29.3538	-26:18:43.385
J1024-0052	10:24:29.5865	-00:52:55.499
J1024-0052	10:24:29.5866	-00:52:55.499
J1035-2011	10:35:02.1553	-20:11:34.359
J1037-2934	10:37:16.0797	-29:34:02.812
J1048-1909	10:48:06.6204	-19:09:35.726
J1058+0133	10:58:29.6052	+01:33:58.824
J1127-1857	11:27:04.3924	-18:57:17.440
J1130-1449	11:30:07.0526	-14:49:27.387
J1133+0040	11:33:20.0558	+00:40:52.838
J1146-2447	11:46:08.1034	-24:47:32.896
J1147-0724	11:47:51.5540	-07:24:41.140
J1246-0730	12:46:04.2321	-07:30:46.574
J1246-2547	12:46:46.8020	-25:47:49.287
J1256-0547	12:56:11.1665	-05:47:21.524
J1305-1033	13:05:33.0150	-10:33:19.427
J1316-3338	13:16:07.9860	-33:38:59.171
J1337-1257	13:37:39.7828	-12:57:24.692
J1357-1527	13:57:11.2450	-15:27:28.785
J1408-0752	14:08:56.4812	-07:52:26.665
J1438-2204	14:38:09.4694	-22:04:54.746
J1448-1620	14:48:15.0542	-16:20:24.548
J1512-0905	15:12:50.5329	-09:05:59.828
J1522-2730	15:22:37.6760	-27:30:10.784
J1557-0001	15:57:51.4340	-00:01:50.413
J1625-2527	16:25:46.8916	-25:27:38.326
J1700-2610	17:00:53.1541	-26:10:51.724
J1709-1728	17:09:34.3454	-17:28:53.364
J1733-1304	17:33:02.7058	-13:04:49.547
J1743-0350	17:43:58.8561	-03:50:04.616
J1820-2528	18:20:57.8509	-25:28:12.587
J1911-2006	19:11:09.6529	-20:06:55.108
J1939-1525	19:39:26.6577	-15:25:43.057
J1939-1002	19:39:57.2562	-10:02:41.519
J2000-1748	20:00:57.0904	-17:48:57.672
J2040-2507	20:40:08.7729	-25:07:46.662
J2129-1538	21:29:12.1759	-15:38:41.040
J2134-0153	21:34:10.3096	-01:53:17.238
J2158-1501	21:58:06.2819	-15:01:09.327
J2236-1433	22:36:34.0871	-14:33:22.188
J2255-0844	22:55:04.2398	-08:44:04.021
J2258-2758	22:58:05.9629	-27:58:21.255
J2323-0317	23:23:31.9537	-03:17:05.023
J2331-1556	23:31:38.6525	-15:56:57.008
J2333-2343	23:33:55.2379	-23:43:40.657
J2337-0230	23:37:57.3391	-02:30:57.628
J2348-1631	23:48:02.6085	-16:31:12.021
J2358-1020	23:58:10.8824	-10:20:08.610

TABLE 2  
ASTROMETRIC CHECK SOURCES AND THEIR ASSUMED POSITIONS.

J2000 Name	Right Ascension (J2000)	Declination (J2000)
J0115-0127	01:15:17.09996	-01:27:04.5762
J0437-1844	04:37:01.48273	-18:44:48.6118
J0513-2159	05:13:49.11433	-21:59:16.0898
J0539-2839	05:39:54.28146	-28:39:55.9462
J0541-0541	05:41:38.08340	-05:41:49.4281
J0609-1542	06:09:40.94956	-15:42:40.6709
J0650-1637	06:50:24.58188	-16:37:39.7239
J0725-0054	07:25:50.63993	-00:54:56.5436
J0808-0751	08:08:15.53602	-07:51:09.8851
J0836-2016	08:36:39.21532	-20:16:59.5033
J0927-2034	09:27:51.82431	-20:34:51.2308
J1150-0023	11:50:43.87078	-00:23:54.2037
J1354-0206	13:54:06.89530	-02:06:03.1896
J1404-0130	14:04:45.89571	-01:30:21.9475
J1405+0415	14:05:01.11983	+04:15:35.8204
J1432-1801	14:32:57.69057	-18:01:35.2468
J1507-1652	15:07:04.78693	-16:52:30.2655
J1513-1012	15:13:44.89339	-10:12:00.2633
J1517-2422	15:17:41.81320	-24:22:19.4754
J1626-2951	16:26:06.02092	-29:51:26.9702
J2011-1546	20:11:15.71093	-15:46:40.2523
J2131-1207	21:31:35.26173	-12:07:04.7957
J2146-1525	21:46:22.97935	-15:25:43.8843
J2229-0832	22:29:40.08431	-08:32:54.4342
J2246-1206	22:46:18.23198	-12:06:51.2769
J2354-1513	23:54:30.19516	-15:13:11.2114



TABLE 3  
(ABRIDGED) CATALOG OF COMPACT RADIO SOURCES MEASURED AT 8.4 GHz.

J2000 Name	Right Ascension (J2000)	Declination (J2000)	$S_{8.4 \text{ GHz}}^{\text{total}}$ (mJy)	$S_{8.4 \text{ GHz}}^{\text{peak}}$ (mJy beam $^{-1}$ )	Comment
J0001-1551	00:01:05.3268	-15:51:07.065	293.4	289.7	VCS1
J0003-1927	00:03:18.6764	-19:27:22.342	244.4	235.5	VCS1
J0004-1148	00:04:04.9139	-11:48:58.378	645.7	629.5	VCS1
J0005-1648	00:05:17.9312	-16:48:04.650	294.6	291.4	VCS1
J0008-2339	00:08:00.3710	-23:39:18.125	383.3	379.5	VCS1
J0008-2559	00:08:26.2527	-25:59:11.538	377.0	373.9	VCS1
J0010-2157	00:10:53.6520	-21:57:04.179	362.4	354.2	VCS1
J0013-0423	00:13:54.1308	-04:23:52.287	251.3	249.4	VCS1
J0015-1812	00:15:02.4937	-18:12:50.913	387.3	379.8	VCS1
J0016-2343	00:16:05.7393	-23:43:52.161	103.3	99.3	
J0022+0014	00:22:25.4257	+00:14:56.164	625.2	597.7	
J0024-0412	00:24:45.9816	-04:12:01.522	324.9	306.7	VCS1
J0030-0211	00:30:31.8233	-02:11:56.122	184.6	180.7	
J0031-1426	00:31:56.4109	-14:26:19.366	156.1	151.9	
J0034-2303	00:34:54.7960	-23:03:35.221	126.7	125.1	
J0037-2145	00:37:14.8247	-21:45:24.681	173.7	172.8	
J0038-2459	00:38:14.7287	-24:59:02.111	397.6	390.0	VCS1
J0038-2120	00:38:29.9540	-21:20:03.977	222.7	205.2	VCS1
J0051-0650	00:51:08.2114	-06:50:02.218	800.2	777.0	VCS1
J0053-0727	00:53:36.5168	-07:27:29.604	172.6	166.2	
J0058-0539	00:58:05.0680	-05:39:52.258	538.3	522.7	VCS1
J0101-2831	01:01:52.3891	-28:31:20.446	220.3	216.7	VCS1
J0102-2646	01:02:56.3546	-26:46:36.530	164.5	158.3	
J0104-2416	01:04:58.2064	-24:16:28.444	240.8	240.1	VCS1
J0106-2718	01:06:26.0816	-27:18:11.837	699.3	695.7	VCS1
J0110-0741	01:10:50.0235	-07:41:41.110	498.6	496.0	VCS1
J0115-2804	01:15:23.8834	-28:04:55.221	669.1	656.8	VCS1
J0117-1507	01:17:38.9287	-15:07:55.023	76.3	68.3	
J0117-2111	01:17:48.7839	-21:11:06.617	329.0	325.9	VCS1
J0118-2141	01:18:57.2655	-21:41:30.112	570.5	541.1	VCS1
J0122-0018	01:22:13.9078	-00:18:01.050	196.9	181.7	
J0125-0005	01:25:28.8418	-00:05:55.925	1308.9	1250.6	VCS1
J0131-1211	01:31:12.5474	-12:11:00.688	87.0	82.1	
J0132-1654	01:32:43.4824	-16:54:48.459	1150.8	1056.6	
J0134+0003	01:34:12.7061	+00:03:45.125	315.9	304.8	
J0135-2008	01:35:37.5123	-20:08:45.848	735.0	717.0	VCS1
J0138-0540	01:38:51.8529	-05:40:08.213	222.8	217.3	VCS1
J0138-2254	01:38:57.4664	-22:54:47.335	236.6	226.7	VCS1
J0142-1714	01:42:23.4059	-17:14:35.446	122.6	120.4	
J0142-0544	01:42:38.8785	-05:44:01.518	186.0	174.7	
J0145-2733	01:45:03.3913	-27:33:34.301	635.2	627.9	VCS1
J0147-2144	01:47:07.3509	-21:44:42.525	82.6	77.9	
J0151-1732	01:51:06.0827	-17:32:44.730	347.6	338.8	VCS1
J0151-1719	01:51:48.0489	-17:19:55.070	125.3	123.7	
J0152-1412	01:52:32.0148	-14:12:39.397	289.4	262.8	VCS1
J0153-1906	01:53:01.5096	-19:06:56.702	126.4	123.4	
J0154-2329	01:54:46.1008	-23:29:53.908	123.2	118.6	
J0206-2212	02:06:20.0700	-22:12:19.615	214.8	201.7	VCS1
J0210-1444	02:10:23.1773	-14:44:58.996	177.8	174.8	
J0215-0222	02:15:42.0155	-02:22:56.757	596.7	581.2	VCS1
J0217-0820	02:17:02.6612	-08:20:52.315	332.1	323.9	VCS1
J0217-0121	02:17:54.9976	-01:21:50.724	94.8	91.6	
J0217-1631	02:17:57.2494	-16:31:10.448	375.8	371.5	VCS1
J0219-1842	02:19:21.1601	-18:42:38.723	415.9	410.1	VCS1
J0220-2151	02:20:35.1475	-21:51:12.055	235.8	231.8	VCS1
J0222-1615	02:22:00.7252	-16:15:16.522	434.3	421.9	VCS1
J0223-1656	02:23:43.7634	-16:56:37.685	192.9	191.3	
J0226-1843	02:26:47.6274	-18:43:39.209	210.1	200.6	
J0227-0621	02:27:44.4625	-06:21:06.741	176.2	169.3	
J0239-1348	02:39:26.0230	-13:48:43.345	188.0	185.2	
J0239-0234	02:39:45.4714	-02:34:40.925	812.8	802.7	
J0240-0504	02:40:56.1720	-05:04:42.200	150.1	145.2	
J0243-0550	02:43:12.4692	-05:50:55.295	607.0	604.9	VCS1
J0246-1236	02:46:58.4706	-12:36:30.786	357.7	348.2	VCS1
J0252-2219	02:52:47.9544	-22:19:25.421	406.1	398.0	VCS1
J0256-2137	02:56:12.8401	-21:37:29.099	267.1	244.9	VCS1
J0259-0019	02:59:28.5152	-00:19:59.981	824.7	812.3	VCS1
J0301-1812	03:01:06.7171	-18:12:17.844	101.6	100.9	
J0303-2407	03:03:26.5007	-24:07:11.464	210.1	186.7	
J0315-1031	03:15:56.8729	-10:31:39.409	192.9	182.9	
J0325-2415	03:25:13.3422	-24:15:48.053	302.4	301.2	VCS1
J0327-2202	03:27:59.9234	-22:02:06.403	515.1	485.2	VCS1
J0329-2357	03:29:54.0746	-23:57:08.789	511.1	501.7	VCS1
J0331-2524	03:31:08.9185	-25:24:43.300	175.0	174.2	
J0339-1736	03:39:13.7048	-17:36:00.785	69.9	66.8	
J0340-2152	03:40:03.4097	-21:52:01.387	103.3	88.1	
J0349-2401	03:49:15.3891	-24:01:14.313	90.5	85.5	
J0349-2102	03:49:57.8272	-21:02:47.730	259.0	252.9	VCS1
J0357-0751	03:57:43.2936	-07:51:14.555	329.6	324.8	VCS1